29

Prediction of Airfoil Stall by Using Launder-Sharma Turbulence Model

Zhong Lei *, Toshiyuki Iwamiya †

Abstract Simulations are conducted to investigate the capabilities of the low-Re $k-\epsilon$ model in predicting aerodynamic characteristics of the static stall airfoil. Launder-Sharma model[2], which represents typically a kind of the low-Re two-equation $k-\epsilon$ model, is tested. Results show that in the computation of the trailing-edge stall, low-Re two-equation model delays the stall angle and underpredicts the peak lift as compared with experimental data. The separation region is also underpredicted due to the computation of fully turbulent flow everywhere. Generally, the computational results agree well with the experiment qualitatively.

1 INTRODUCTION

The aerodynamic characteristics of the airfoil are an important consideration for the optimization of the performance and, therefore, the design of wing configuration of the aircraft. According to McCullough and Gault [1], there are three types of static stall: trailing-edge stall, thin-airfoil stall, and leading-edge stall. Trailing-edge stall is characterized by the forward movement of the separation point. Thin-airfoil stall is preceded by laminar flow separation at the leading-edge with turbulent reattachment at a point downstream that moves rearward with increasing the angle of attack. The closed separation region is commonly referred to a long separation bubble. Leading-edge stall is also preceded by laminar separation near the leading-edge, but reattached the wall immediately as a turbulent flow due to the rapid transition. The difficulties associated with computations of the flowfield of the static stall airfoil are both numerical (accuracy of numerical discretization, numerical stability and grid-independence) and physical (turbulence model and transition model). In most situations, because the Reynolds number is high and the physical diffusion is small, the numerical diffusion should be small enough to avoid unphysical solutions. This results in a requirement of high-order scheme and fine grids in the viscous region. Grids must be fine enough to ensure a reliable solution, and at the meantime, the space size should not be too small in order to maintain the efficiency of calculation. The other difficulty is the lack of physical understanding of turbulence and laminar-turbulent transition phenomenon. Although most of current turbulence models are encouraging in predicting engineering application flows, they cannot accurately compute complex flows, especially with separation, for example, the stall characteristics of the airfoil flow [4]. And the difficulty of laminar-turbulent transition phenomenon prevents correct prediction of the transition process [5]. This makes the accurate prediction particularly difficult.

In the present work, the Reynold-averaged Navier-Stokes (RANS) equations are used with combination of the two-equation $k-\epsilon$ turbulence model. Launder-Sharma models are tested because it has been widely accepted and used in many engineering applications. It employs a damping factor that represents a general property of low-Re flows (e.g. turbulent Reynolds number R_T), and are more appropriate than ones that introduce a dependence on wall-proximity (y^+, R_y, R_ϵ), for computation of flowfields about complex configurations.

The purpose of the present work is to assess the performance of the low-Re $k-\epsilon$ model when applied to the flows of the static stall airfoil. It will focus on the prediction of aerodynamic characteristics, including lift, drag, moment and pressure distributions at the wall. Due to the difficulty of modeling the turbulent transition process, fully turbulent computations are conducted in this work. There is not any transition model used in the computation.

This work was presented in the Workshop [6] held in Tokyo, June 2000, that discussed the capability of CFD in predicting static stall of the airfoil. The test were assigned to work on the experiment of airfoil flows carried out by McCullough and Gault [1].

*VINAS Co. Ltd., Osaka, Japan, lei@nal.go.jp
†National Aerospace Laboratory, Tokyo, Japan, iwamiya@nal.go.jp

2 TURBULENCE MODEL

The governing equations of the flow field are taken to be steady compressible two-dimensional Reynold-averaged Navier-Stokes (RANS) equations. These equations contain the turbulent second-moment correlation tensor, so-called Reynolds stresses $\tau_{ij} = \rho\overline{u_i' u_j'}$. For the requirement of closure, Boussinesq approximation assumed a linear eddy-viscosity hypothesis for the turbulent Reynolds stresses.

$$\tau_{ij} = -\rho\overline{u_i' u_j'} = 2\mu_T\left(S_{ij} - \frac{1}{3}\frac{\partial \overline{u}_k}{\partial x_k}\delta_{ij}\right) - \frac{2}{3}\rho k\delta_{ij} \quad (1)$$

The two-equation models solve an equation for the turbulent kinetic energy k to get a velocity scale. They also solve an equation for a parameter related to a length scale. In most of widely used $k-\epsilon$ models, the other equation is defined for the turbulent dissipation ϵ.

$$\overline{u}\frac{\partial k}{\partial x} + \overline{v}\frac{\partial k}{\partial y} = P_k - (\tilde{\epsilon} + \epsilon_0) + \frac{\partial}{\partial x_j}\left[\left(\nu + \frac{\nu_T}{\sigma_k}\right)\frac{\partial k}{\partial x_j}\right] \quad (2)$$

$$\overline{u}\frac{\partial \tilde{\epsilon}}{\partial x} + \overline{v}\frac{\partial \tilde{\epsilon}}{\partial y} = C_{\epsilon 1} f_1 \frac{\tilde{\epsilon}}{k} P_k - C_{\epsilon 2} f_2 \frac{\tilde{\epsilon}^2}{k} + E + \frac{\partial}{\partial x_j}\left[\left(\nu + \frac{\nu_T}{\sigma_\epsilon}\right)\frac{\partial \tilde{\epsilon}}{\partial x_j}\right] \quad (3)$$

where

$$P_k = \tau_{ij}\frac{\partial \overline{u}_i}{\partial x_j}$$

and the dissipation, ϵ, is related to the quantity $\tilde{\epsilon}$, which is called dilatation dissipation, by

$$\epsilon = \epsilon_0 + \tilde{\epsilon}$$

The eddy-viscosity is defined as

$$\nu_T = C_\mu f_\mu \frac{k^2}{\tilde{\epsilon}} \quad (4)$$

Five empirical damping functions, f_1, f_2, f_μ, ϵ_0 and E are contained in models. These functions depend upon one or more of the following dimensionless parameters.

$$R_T = \frac{k^2}{\tilde{\epsilon}\nu}, \quad (5)$$

Launder-Sharma Model (1974) [2] defines them as follows

$$f_\mu = e^{-3.4/(1.0+R_T/50)^2}, \quad f_1 = 1.0,$$
$$f_2 = 1.0 - 0.3e^{-R_T^2},$$
$$\epsilon_0 = 2\nu\left(\frac{\partial\sqrt{k}}{\partial n}\right)^2, \quad E = 2\nu\nu_T\left(\frac{\partial^2 U}{\partial n^2}\right)^2, \quad (6)$$
$$C_{\epsilon 1} = 1.44, \quad C_{\epsilon 2} = 1.92, \quad C_\mu = 0.09,$$
$$\sigma_k = 1.0, \quad \sigma_\epsilon = 1.3.$$

where n means the normal direction of the surface.

To prevent the normal Reynolds stresses ($\overline{u'^2}$ and $\overline{v'^2}$) from negative values, a clipping operation (i.e., to set normal stresses equal to zero if they become negative) is introduced.

$$\begin{aligned} \tau_{xx} &= -\rho\overline{u^2} = 0, \quad \text{if} \quad \tau_{xx} > 0 \\ \tau_{yy} &= -\rho\overline{v^2} = 0, \quad \text{if} \quad \tau_{yy} > 0 \end{aligned} \quad (7)$$

The boundary conditions for the turbulence model were set to be zero at the wall.

$$k = \epsilon = 0 \qquad \text{at wall} \quad (8)$$

In the field far away from the boundary layer flow, the turbulent flow behaves like an isotropic turbulence decayed in freestream. The turbulence equation (2) and (3) reduce to a set of coupled ordinary differential equations as all of the cross-stream derivatives vanish.

$$U_e\frac{dk_e}{dx} = -\epsilon_e \quad (9)$$

$$U_e\frac{d\epsilon_e}{dx} = -C_{\epsilon 2} f_2 \frac{\epsilon_e^2}{k_e} \quad (10)$$

Thus k and ϵ can be solved from these equations once the values of both k and ϵ are specified at inflow points. At outflow points they are both extrapolated from the interior region.

The nonreflective Riemann boundary condition was used flow variables at far field boundary. At the wall, the non-slip condition was used for the velocities, and the pressure was calculated from a generalized normal momentum equation.

3 NUMERICAL METHOD

Both the Reynolds-averaged Navier-Stokes (RANS) equations, and the set of turbulence model equations are solved by a LU-ADI method (Obayashi [3] et al 1986) for the convective terms. This is an implicit time integration scheme that each ADI operator is rewritten in the diagonal form, and the flux-vector

splitting technique is applied. In turbulence model equations, the source terms are treated implicitly to guarantee a rapid convergence rate. Among the explicit terms of the right-hand side, the convective terms are discretized using the third-order upwind-biased scheme of the MUSCL approach. Diffusion and source terms are discretized with the central difference scheme.

In the present computation, the initial grids are generated by using the hyperbolic partial differential equation method of a commercial software GRIDGEN. For the flow of the airfoil NACA$63_3 - 018$, C-type grids with 358×140 grids in the streamwise and in the normal direction to the surface, respectively, are constructed in the computational region. Grids are clustered near the wall. The spatial distance of the first grid point away from the wall is restricted to be less than 5.0×10^{-6} and this gurantees $y^+ = (u_\tau)\, y/\nu$ to be less than 0.5 in all stations, where $u_\tau = \sqrt{(\tau_{xy} + t_{xy})/\rho}$. Within the boundary layer, the number of grids is more than 100. Under this fine grid, low-Re models can be integrated to the wall without any need of two-layer treatment. The initial grids are automatically changed according to different angles of attack in the computation. An example for the case of $\alpha = 15°$ is shown in Fig.1. Grid points on the airfoil are fixed in all cases, while the outer boundary is rotated and the wake-cut line is curved as the angle of attack changed

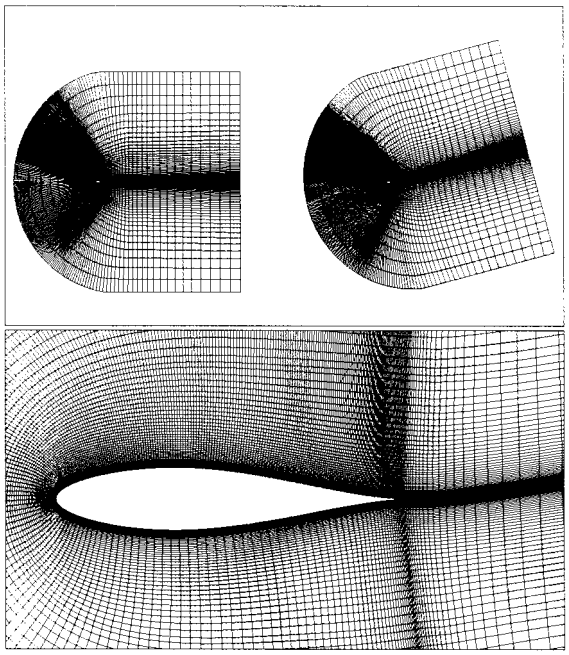

Figure 1: Grids around the airfoil.

4 RESULTS AND DISCUSSION

Calculations have been performed for experimental data of trailing-edge stall, which were obtained on an NACA$63_3 - 018$ airfoil by McCullough and Gault (1955). Because of the numerical difficulties, leading-edge stall and thin-airfoil stall have not been calculated yet and will be done in future. Reynolds number, which was based on the free-stream conditions and the airfoil chord, was 5.8×10^6 for all angles of attack. Since the tunnel turbulence level was not measured in the experiment, the turbulence intensity was assumed. In the freestream, we assumed the turbulence intensity to be 2%, and the turbulent viscosity to be 2.0. It was also found that at this level, the solution was not sensitive to the values of the freestream. To get a good performance of the compressible code, computations were conducted at Mach number 0.2.

No attempt was made to simulate transition and the flowfield was treated as fully developed turbulence for all cases. Aerodynamic force coefficients for all cases are shown as functions of the angle of attack α in Fig.2 and compared with experimental data reading from the graph of the literature [1]. Two sets of experimental data were compared in this study. One was the original data that have not been corrected for tunnel-wall constraint or the effects of compressibility, and the other was the data corrected by using the method described in the appendix A of the literature [1].

$$\begin{aligned} \alpha &= \alpha_u + 0.475 C_{l_u} + 1.902 C_{m_u}, \\ C_l &= 0.916 C_{l_u}, \end{aligned} \tag{11}$$

where the subscript u denotes the uncorrected coefficients presented in [1]. Because the wall boundaries of the tunnel required the flow to turn to parallel to the walls and the outer flow was modified. It made the data different from what obtained in an open field while the computation is usually conducted in a free field. The computation predicted the abrupt onset of stall to be $\alpha = 14.5°$. It was a little later than that of the uncorrected data, but when compared with the corrected data, it agreed very well with not only the abrupt onset of stall but also the peak lift. In the computation, the flow remained attached to the wall

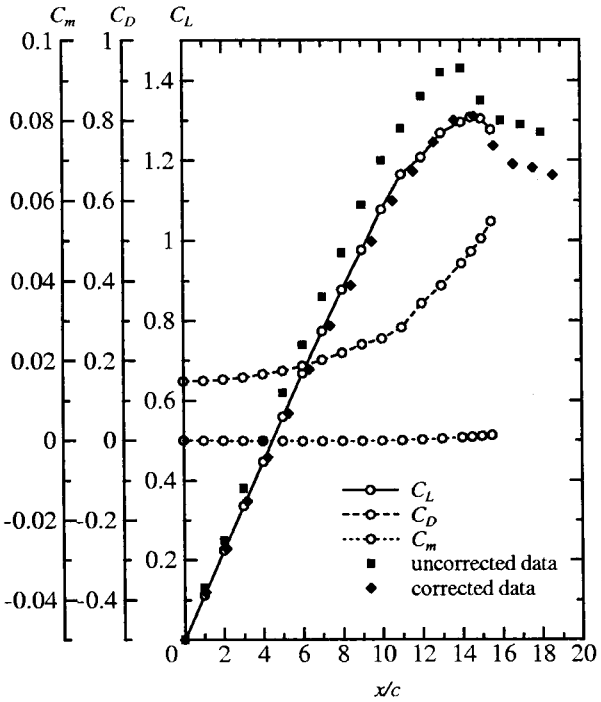

(a) variations of C_l, C_d and C_m with α

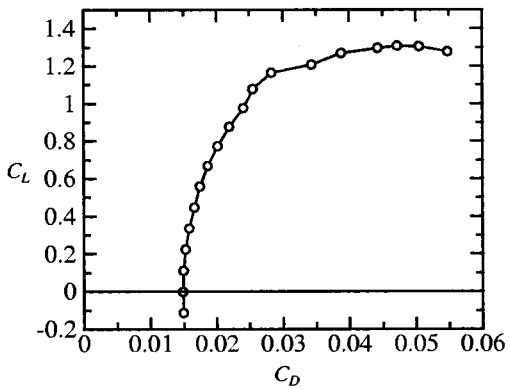

(b) variations of C_l and C_d

Figure 2: Aerodynamic characteristics of the airfoil.

until an angle of about 12° as shown in Fig.4. There were some variation in the forces at the point of 12°. With further increase of the angle of attack, a separation region, so-called long bubble, was appeared. The extent of the long bubble moved progressively forward. The computation predicted a smaller separation region than that of experiments. It was resulted from overprediction of the eddy-viscosity due to the computation of fully turbulent flows everywhere. The separation region was suppressed by the energy extracted from the mean flow by turbulent motion. This suggests that turbulent transition should be correctly predicted to get reliable results. Above an angle of attack of 16°, no steady solutions were obtainable with Launder-Sharma model because vortexes started to be shed unsteadily from the trailing-edge.

Representative pressure distribution are presented in Fig.3. At high angles of attack, the large plateau pressure resulting from separation was well reproduced by the model. The pressure suction peaks were also reasonably high. Near the leading-edge, the eddy-viscosities were small and turbulence was weak. The flow was in a laminar-like situation. In Fig.4, it is shown that the computational results of low-Re model produced a sudden increase of friction coefficients C_f. This result is very similar to the computation of bypass transition. It indicates that with the low-Re behavior of turbulence model, we have actually conducted a computation of bypass transitional flow. When turbulence intensity and turbulent dissipation were adjusted to follow a natural laminar-turbulent transition, no significant change was found. The locations of sudden increase of C_f were almost fixed at $x/c = 4\%$ on the upper surface, and independent on the turbulence level of freestream and angle of attack. However, this 'transition point' was predicted too early.

Typical flow patterns are shown in Fig.5, where streamlines are plotted. Separation region was reproduced above the angle of attack of 12°. At the stall angle of attack, the separation region covers more than 30% of the chord. A large recirculation was apparently observed. One of the most important quantity for turbulence computation, the eddy-viscosities are then shown in Fig.6. Once again, one can find that the turbulence is very weak at the beginning of turbulence development, increased gradually and undergoes transition to fully turbulent flow at the location about

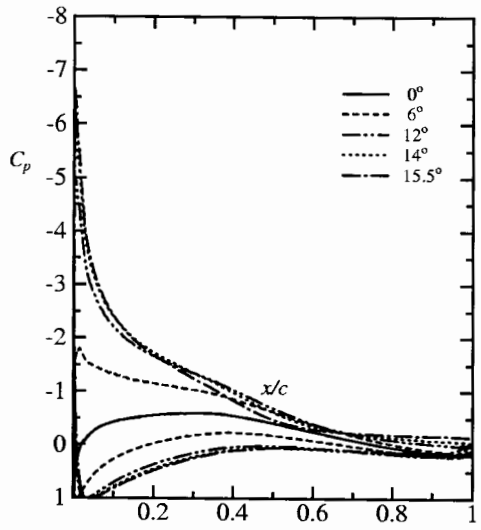

Figure 3: Computational results of pressure distribution on the NACA$63_3 - 018$.

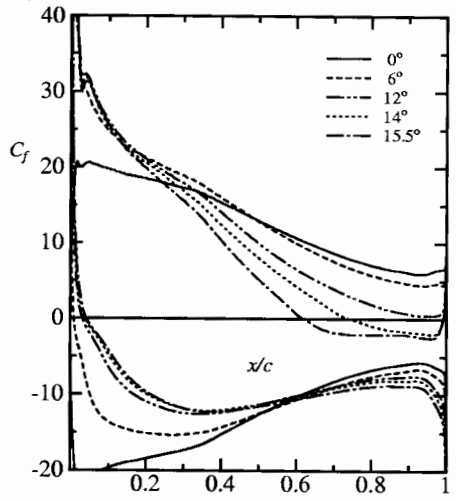

Figure 4: Computational results of friction distribution on the NACA$63_3 - 018$.

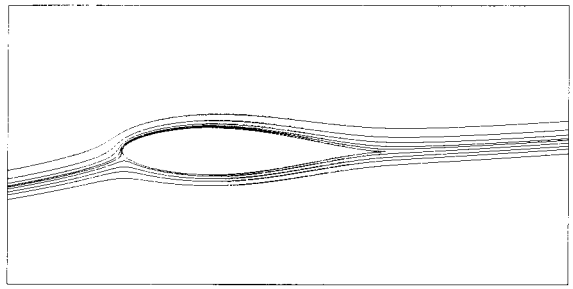

(a) $\alpha = 6.0$

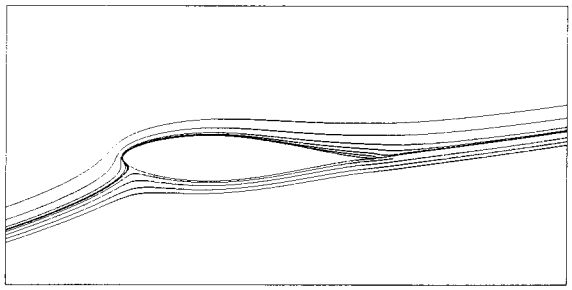

(b) $\alpha = 12.0$

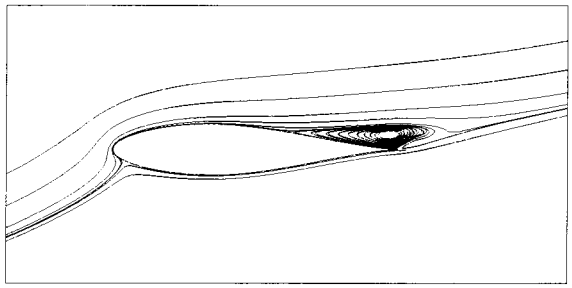

(c) $\alpha = 15.5$

Figure 5: Flow patterns of streamline.

$x/c = 4\%$. Turbulence was expanded outward as the angle of attack was increased.

5 CONCLUSION REMARKS

Flows of trailing-edge stall of the NACA$63_3 - 018$ airfoil have been computed with Launder-Sharma $k - \epsilon$ model. For this case, although the abrupt onset of stall was delayed by the computation and the maximum lift were underpredicted when compared with the uncorrected experimental data, it agreed reasonably well when compared with the corrected experimental data. The extent of separation region was underestimated due to the computation of fully turbulent flow everywhere.

It is somewhat disappointing that, the low-Re number $k - \epsilon$ model failed in predicting correct transition points of natural turbulent transition although it has had some success for bypass transitional flows.

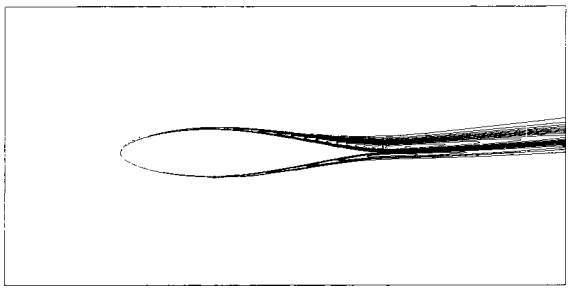

(a) $\alpha = 6.0$

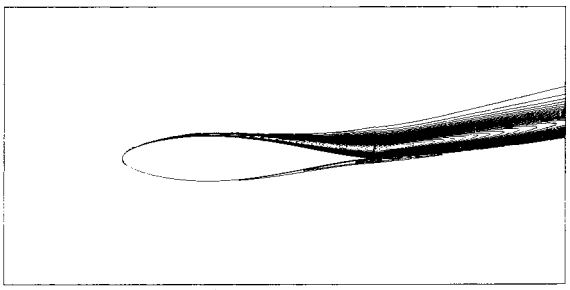

(b) $\alpha = 12.0$

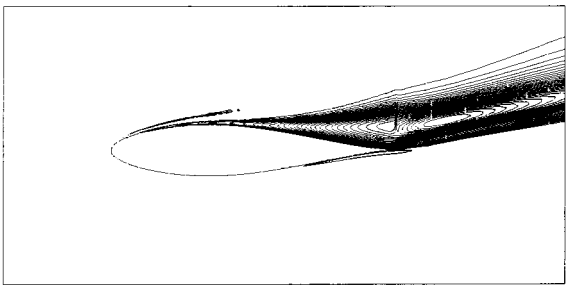

(c) $\alpha = 15.5$

Figure 6: Distribution of the turbulent eddy-viscosity.

Another important problem is that the experimental conditions, such as the Mach number, turbulence values of free stream, are not available in the literature [1]. Actually, the computation conditions were determined by the authors' experience, and they were not completely as the same as the corresponding experiment.

Because of the lack of detail experimental data of Reynolds stresses, it is impossible to assess turbulence model further with comparison.

So, even though the lift was well predicted in this study, because of the reason mentioned above, it is still doubtful that the Launder-Sharma model is really capable of predicting trailing-edge stall of airfoil.

References

[1] McCullough, G.B. and Gault, D.E., 1951, "Examples of Three Representative Types of Airfoil-Section Stall at Low Speed," NACA TN 2502.

[2] Launder, B.E. and Sharma, B.I., 1974, "Application of the Energy-Dissipation Model of Turbulence to the Calculation of Flow near a Spinning Disc," *Letters in Heat and Transfer*, Vol.I, No.2, pp131-138.

[3] Obayashi, S., Matsushima, K., Fujii, K. and Kuwahara, K., 1986, "Improvements in Efficiency and Reliability for Navier-Stokes Computations Using LU-ADI Factorization Algorithm," AIAA Paper 86-338.

[4] Rizzetta, D.P. and Visbal, M.R., 1992, "Comparative Numerical Study of Two Turbulence Models for Airfoil Static and Dynamic Stall," AIAA paper 92-4649

[5] Savill, A.M., 1996, "One-Point Closures Applied to Transition," in *Turbulence and Transition Modelling*, Hällback, M. et al eds., Kluwer Academic Publisher, pp233-268.

[6] *Proceedings of the NAL Symposium on Numerical Simulation Techniques in Aerospace 2000*, National Aerospace Laboratory, Tokyo, June 2000.